CrossMark

ORIGINAL PAPER

First-Principle Study of Electronic and Half-Metallic Ferromagnetic Properties of Vanadium (V)-Doped Cubic BP and InP

Miloud Boutaleb[1,2] · Bendouma Doumi[2] · Allel Mokaddem[3] · Adlane Sayede[4] · Abdelkader Tadjer[1]

Abstract In this study, we use the first-principle calculations of density functional theory with gradient generalized approximation of Wu–Cohen to investigate the doping effect of vanadium impurity on structural, electronic and magnetic properties of $In_{1-x}V_xP$ and $B_{1-x}V_xP$ alloys at various concentrations $x = 0.0625$, 0.125 and 0.25. Owing to the metallic nature of majority spin and semiconducting minority spin, the $In_{1-x}V_xP$ compounds exhibit a half-metallic character with total magnetic moments of $2\ \mu_B$, while the $B_{1-x}V_xP$ has metallic nature for all concentrations. The results of exchange parameters revealed that exchange coupling between vanadium atoms and the conduction band is ferromagnetic, confirming the magnetic feature of $In_{1-x}V_xP$ and $B_{1-x}V_xP$. From our findings, we have predicted that the $In_{1-x}V_xP$ alloys seem to be potential materials for spintronics.

Keywords Electronic structures · p-d exchange coupling · Half-metallic ferromagnetism

✉ Miloud Boutaleb
mbouttaleb@yahoo.fr

1 Modelling and Simulation in Materials Science Laboratory, Physics Department, Djillali Liabes University of Sidi Bel-Abbes, 22000 Sidi Bel-Abbes, Algeria

2 Faculty of Sciences, Dr. Tahar Moulay University of Saida, 20000 Saida, Algeria

3 Centre Universitaire Nour Bachir El Bayadh, 32000 El Bayadh, Algérie

4 Unité de Catalyse et Chimie du Solide (UCCS), UMR CNRS 8181, Faculté des Sciences, Université d'Artois, Rue Jean Souvraz, SP 18, 62307 Lens, France

1 Introduction

Over the last few years, the III-V semiconductor materials have been extensively studied as potential candidates for new spintronics applications [1, 2]. These materials in the binary structure are composed by one atom of boron group (B, Al, Ga, In) and one atom of pnictogen groups (N, P, As, Sb). The semiconductor materials used in electronic devices are doped under precise conditions to control the concentration and regions of dopants. The parsimonious introduction of $3d$-transiton metal atoms as doping magnetic fraction in the binary structures is a novel field of study known as the diluted magnetic semiconductor compounds (DMSs) [3, 4].

Indium phosphide (InP) and boron phosphide (BP) semiconductors form covalent crystals with some two different ionic characters of bonds. The boron or indium with phosphorus atoms shares their valence electrons forming sp3 hybrid orbitals. These hybrid orbitals separate the bonding orbitals that are filled with electrons forming the valence band (VB) and the anti-bonding orbitals that are empty at 0 K and form the conduction band (CB) by a band gap containing no electronic states. [5, 6] The values of energy band gaps and the lattice parameters of these crystals are obtained according to the difference in electron affinity of elements by moving an electron from vacuum to the conduction band minimum. The substitution of small proportion of vanadium as magnetically atoms at the B or In cation sites of BP and InP host semiconductors could change the properties of these compounds to ternary DMSs alloys. The nature of chemical bond and the strength of the ionic character of this bond are in well relation with the ferromagnetic feature of DMSs alloys [7, 8]. We note here that the differences in values of electron affinities cause automatically different values of electro-negativities between B and P atoms

and In and P atoms and gives two kinds of polarities of the chemical bond in BP and InP semiconductors. These are clearly observed in the case of InP that's considered as covalent crystal with enhanced ionic character chemical bond. However, BP is recognized as covalent crystal with undersized ionic character chemical bond because it involved the sharing of electron pairs between boron and phosphorus atoms but not delocalized electrons, in which each is covalently bonded to its nearest neighbours.

The diluted magnetic semiconductors are compounds that combine the semiconducting and magnetic properties and exhibit a number of new phenomena, such as non-volatile memory, quantum computing and magneto-optical memory. They are used in spin-electronic and spin-photonic devices [9–14]. The III-V DMSs have prepared experimentally by using the technique of molecular beam epitaxy (MBE) under low growth at temperatures in the range of 200 to 300 °C [15–17]. We can prove the existence of ferromagnetism by changing the magnetic phase with using light in (In.Mn)As/(Al,Ga)Sb [18–20]. The famous property that makes revolutions in spintronic is the stability of ferromagnetism described by the Zener model [21]. Extensive theoretical studies have been discussed this phenomenon in III-V DMSs and investigate their half-metallic ferromagnetic behaviour. They conclude that III-V DMSs are from the better candidates of spintronic applications [22–35]

InP and BP crystallized in a face-centred cubic at zinc-blend structure with space group of $F\bar{4}3m$ and coordinate in tetrahedral symmetry. Their lattice parameters are 5.868 and 4.538 Å, respectively, for InP and BP. The InP has a distance of 0.254 nm as nearest neighbour and direct band gap energy of 1.344 eV at 300 K [36]. It also has one of the longest-lived optical phonons of any compound with the zinc-blend crystal structure [37]. It was used with indium gallium arsenide to make a record-breaking pseudo-morphic hetero-junction bipolar transistor that could operate at 604 GHz [38]. Although, the InP semiconductor is considered a possible candidate as a DMSs material according to the theoretical report [31, 39, 40] and to the experimental results of J. Hollingsworth et al [41]. The BP has an indirect band gap of 2.1 eV at 300 K; it is used as an essential component in light-emitting diodes (LED) and finds applications in the laser diodes [42]. BP is also a very efficient heat conductor with a room-temperature thermal conductivity of 400 W (m K)$^{-1}$ [43].

In this regard, we will study the structural, electronic and magnetic properties of ternary compounds $(In,B)_{1-x}V_xP$ doped with vanadium as impurity of transition metal at various concentrations ($x = 0.0625, 0.125, 0.25$). According to the calculations method of first-principles full-potential linearized augmented plane wave (FP-LAPW) with generalized gradient approximation functional proposed by Wu and Cohen (WC-GGA), we will expect to get the half-metallic

ferromagnetic character in the case of $In_{1-x}V_xP$ but not in the $B_{1-x}V_xP$ DMSs and find out that the ternary compositions of indium phosphide seem to be good candidates for spintronics applications.

2 Method of Calculations

Our calculations are performed with the density functional theory (DFT) [44, 45]. We employed the full-potential linearized augmented plane waves (FP-LAPW) method as implemented in the WIEN2k code [46]. The Wu and Cohen generalized gradient approximation functional (WC-GGA) was used for the exchange correlation potential [47] in order to calculate the electronic and half-metallic ferromagnetic properties of V-doped BP and InP in zinc blend structure, based on $(B,In)_{15}VP_{16}$, $(B,In)_7VP_8$ and $(B,In)_3VP_4$ super cells of 32, 16 and 8 atoms, respectively. We take the muffin–tin radii (R_{MT}) of B, In, P and V as large as possible in such a way that the spheres do not overlap. We have expanded the wave functions in the interstitial region to plane waves with a cutoff of $K_{max} = 8.0/R_{MT}$ (where K_{max} is the magnitude of the largest K vector in the plane wave and R_{MT} is the average radius of the muffin–tin spheres). The maximum value for partial waves inside the atomic sphere was $l_{max} = 10$, while the charge density was Fourier expanded up to $G_{max} = 12$, where G_{max} is the largest vector in the Fourier expansion. For the sampling of the Brillouin zone, ($2 \times 2 \times 5$), ($4 \times 4 \times 2$) and ($4 \times 4 \times 4$) Monkhorst–Pack mesh [48, 49] are utilized for super cells of 32, 16 and 8 atoms, respectively, where the self-consistent convergence of the total energy was at 0.1 mRy.

3 Results and Discussion

The BP and InP crystallize in zinc-blend (B3) structure with space group of $F\bar{4}3m(Td)$, where the B^{+3} or In^{+3} cations occupied a face-centred cubic system, it is located at position (0, 0, 0) and P^{-3} anions positioned at the half of tetrahedral sites of this crystal system so it's located at (0.25, 0.25, 0.25) of cubic cell. The number of coordination is 4–4, which is explained by the fact that each cation is surrounded by four phosphorus anions in a tetrahedral structure. We obtain the diluted magnetic semiconductors $(B,In)_{1-x}V_xP$ compounds at concentrations $x = 0.0625$, $x = 0.125$ and $x = 0.25$ by substituting one B or In cation with one vanadium atom in super cells of 32, 16 and 8 atoms, to get the $(B,In)_{0.9375}V_{0.0625}P$ ($1 \times 2 \times 2$) super cell of 32 atoms with $x = 0.0625$ of tetragonal structure with space group $P\bar{4}2m$, $(B,In)_{0.875}V_{0.125}P$ ($1 \times 1 \times 2$) super cell of 16 atoms with $x = 0.125$ of tetragonal structure with space group $P\bar{4}2m$ and $(B,In)_{0.75}V_{0.25}P$ ($1 \times 1 \times 1$) standard unit cell of 8 atoms

Fig. 1 The crystal structures of $(B,In)_{1-x}V_xP$ compounds. **a** $(B,In)_{0.875}V_{0.125}P$ super cell of 16 atoms with $x = 0.125$, **b** $(B,In)_{0.75}V_{0.25}P$ standard unit cell of 8 atoms with $x = 0.25$ and **c** $(B,In)_{0.9375}V_{0.0625}P$ super cell of 32 atoms with $x = 0.0625$
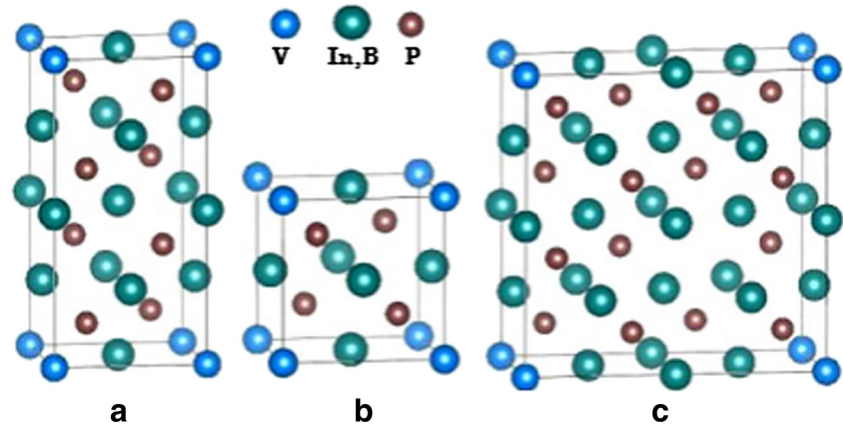
with $x = 0.25$ of cubic structure with space group $F\bar{4}3m$ as shown in Fig. 1.

Through fitting the variation of total energies and equilibrium volumes with the empirical Murnaghan's equation of state [50], we optimize the structural parameters such as lattice constant (a), bulk modulus (B) and its pressure derivative (B') for binaries zinc blend BP, InP and the ternaries alloys of 32 atoms as $(B,In)_{0.9375}V_{0.0625}P$ with 0.0625 concentration, 16 atoms as $(B,In)_{0.875}V_{0.125}P$ with 0.125 concentration and 8 atoms as $(B,In)_{0.75}V_{0.25}P$ with 0.25 concentration of doped vanadium impurity. Our results of structural parameters and various theoretical [31, 51] and experimental [36, 52, 53] data are enumerated in Table 1.

According the contents of Table 1, we note that our results are consistent with the mentioned data. The lattice constant (a), that is defined as the distances between neighbouring unit cells in a three-dimensional lattice, is in good conformity with the experience [36, 52, 53], the difference

in calculation does not exceed one percent and is almost similar with the other theoretical calculations [31, 51]. This parameter lattice is slightly decreasing when the concentration of vanadium increase in the case of $In_{1-x}V_xP$; this is due to the ionic radius of vanadium which is smaller than that of indium atom. But in the case of $B_{1-x}V_xP$, the parameter lattice increases with the increasing of concentration of vanadium due to the small nucleus and the absence of the p-electrons in the nucleus of the boron atom. The calculations of bulk modulus indicate that the compressibility of $In_{1-x}V_xP$ at lower concentration of vanadium (0.0625) is easy then the higher one; this is well explained by the upward trend of bulk modulus with the concentration of vanadium. The DMSs of boron phosphide $B_{1-x}V_xP$ have a different nature than that of indium phosphide $In_{1-x}V_xP$; it is the consequence of a weak ionic character in the chemical bond between boron and phosphorus that is considered as a heterogeneous covalent chemical bond which is far

Table 1 Calculated of lattice constant (a), bulk modulus (B) and its pressure derivative (B') for binary InP, BP and $(B, In)_{1-x}V_xP$ at concentrations ($x = 0.0625, 0.125, 0.25$) of vanadium

Compound	Concentration (x)	a (Å)	B(GPa)	B'	Method
This work					
InP	0.00	5.893	66.55	4.86	WC-GGA
$In_{1-x}V_xP$	0.0625	5.850	67.84	5.19	WC-GGA
	0.125	5.826	70.42	4.62	WC-GGA
	0.25	5.751	74.61	4.77	WC-GGA
BP $B_{1-x}V_xP$	0.00	4.533	167.99	3.89	
	0.0625	4.608	158.47	3.56	
	0.125	4.657	149.92	3.59	
	0.25	4.785	145.40	3.01	
Other calculations					
InP	0.00	5.890 [40]	67.40 [40]		WC-GGA
		5.869 [41]	72.00 [27]		WC-GGA
Bp	0.00	4.538 [56]			experimental
$In_{1-x}V_xP$	0.25	5.888 [26]	61.14 [26]	5.11 [26]	WC-GGA

from being poorly ionic. The first-pressure derivative of bulk modulus (B') has not reached a steady trend with the concentration of vanadium in our alloys.

The substitute of transition metal atom of vanadium impurity in the binary structure of boron and indium phosphide for having the ternary forms of $(B,In)_{1-x}V_xP$ obey at the hybridization of SP3, this under the effect of the surrounding of four anions phosphorus that forms the tetrahedral geometry. The 3d states of vanadium initially degenerate ($V^{+3} \equiv [Ar]4S^0\ 3d^2$) should be separated into two levels totally different in energy ($e_g^2\ t_{2g}^0$). The e_g level of the lowest energy composed by twofold degenerate states ($3d_{x2-y2}$ and $3d_{z2}$) is completely filled; however, the t_{2g} levels characterized with the higher energy are formed by threefold degenerate states ($3d_{xy}$, $3d_{xz}$ and $3d_{yz}$) which are completely empty.

From the curves of spin-polarized total and partial density of states (TDOSs, PDOSs) and the spin-polarized band structures represented in Figs. 2, 3, 4, 5, 6, 7, 8, 9, 10, 11, 12 and 13, respectively, for $In_{0.9375}V_{0.0625}P$, $In_{0.875}V_{0.125}P$, $In_{0.75}V_{0.25}P$, $B_{0.9375}V_{0.0625}P$, $B_{0.875}V_{0.125}P$ and $B_{0.75}V_{0.25}P$ using the WC-GGA approximation of Wu–Cohen [42] at the equilibrium lattice parameter indicated in Table 1, we calculate the spin-minority band gaps E_g (eV) and the half-metallic band gaps G_h (eV) of $In_{1-x}V_xP$ reported in Table 2. It is clear that the 3d-(V) and 3p-(P) states contribute mainly in the Fermi level, having regard the strong p-d hybridization of the tetrahedral symmetry. This will necessarily create bonding states (t^b) at the valence band (VB) and anti-bonding states (t^a) in the dividing gap that cross the Fermi level [54, 55].
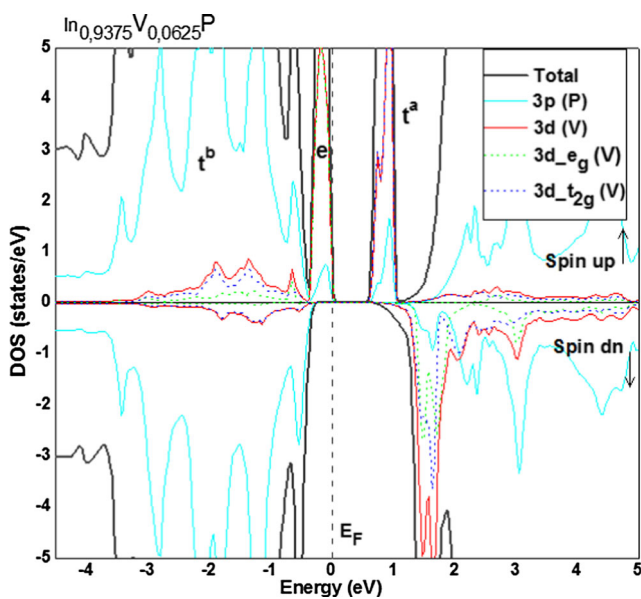

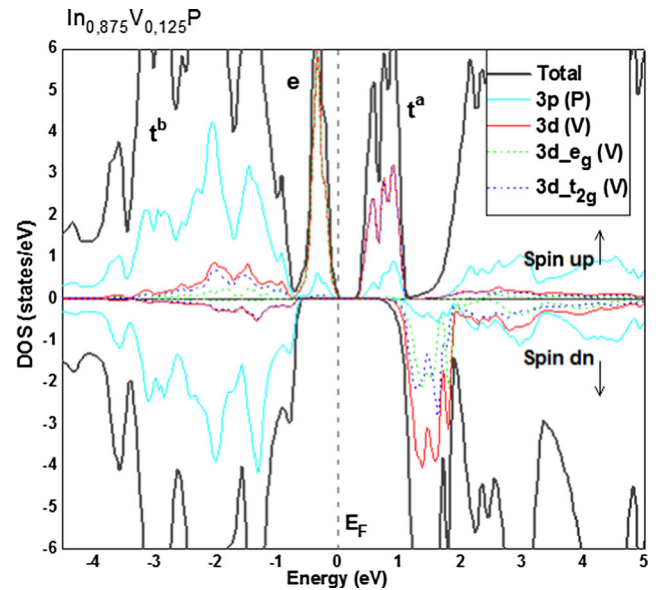**Fig. 3** Spin-polarized total and partial DOS of ($3p$) of P and ($3d$, $3de_g$, $3dt_{2g}$) of V in super cell for $In_{0.875}V_{0.125}P$. The Fermi level is set to zero (*dotted line*)

The total and partial density of states and the band structures of $In_{1-x}V_xP$ alloys represented in Figs. 2, 3, 4, 8, 9 and 10 show that our compounds exhibit a half-metallic ferromagnetic (HMF) property reaching the value of 0.725 eV at 25% of doped vanadium; therefore, $In_{1-x}V_xP$ compounds at all concentration are metallic for majority spin but the minimum of the conduction band cut the Fermi
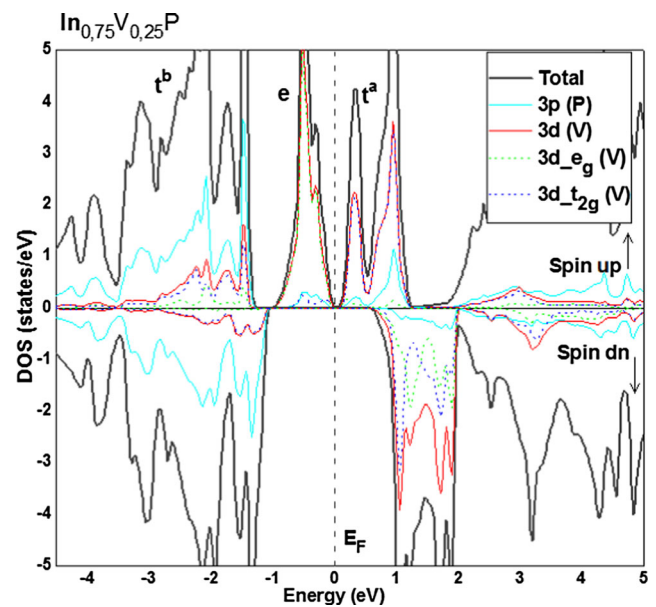

Fig. 2 Spin-polarized total and partial DOS of ($3p$) of P and ($3d\ 3de_g$, $3dt_{2g}$) of V in super cell for $In_{0.9375}V_{0.0625}P$. The Fermi level is set to zero (*dotted line*)
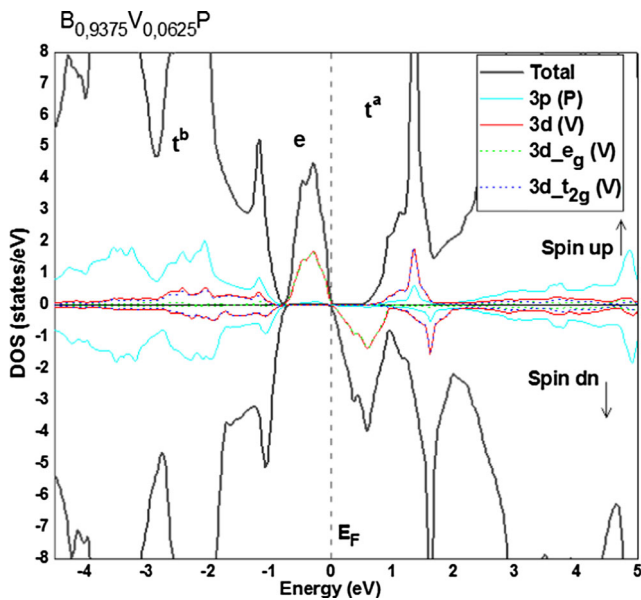

Fig. 4 Spin-polarized total and partial DOS of ($3p$) of P and ($3d$, $3de_g$, $3dt_{2g}$) of V in super cell for $In_{0.75}V_{0.25}P$. The Fermi level is set to zero (*dotted line*)

Fig. 5 Spin-polarized total and partial DOS of $(3p)$ of P and $(3d, 3de_g, 3dt_{2g})$ of V in super cell for $B_{0.9375}V_{0.0625}P$. The Fermi level is set to zero (*dotted line*)

Fig. 6 Spin-polarized total and partial DOS of $(3p)$ of P and $(3d, 3de_g, 3dt_{2g})$ of V in super cell for $B_{0.875}V_{0.125}P$. The Fermi level is set to zero (*dotted line*)

Fig. 7 Spin-polarized total and partial DOS of $(3p)$ of P and $(3d, 3de_g, 3dt_{2g})$ of V in super cell for $B_{0.75}V_{0.25}P$. The Fermi level is set to zero (*dotted line*)

level for minority spin, which have a clear gap. The half-metallic gap is a very important parameter in spintronic; it is defined as the maximum between the lowest energy of the spin-up and spin-down conduction bands with respect to the Fermi level and the absolute values of the highest energy of the spin-up and spin-down valence bands [56, 57]. Also the consequence of the ferromagnetism in the V-doped InP follows from the Zener double exchange
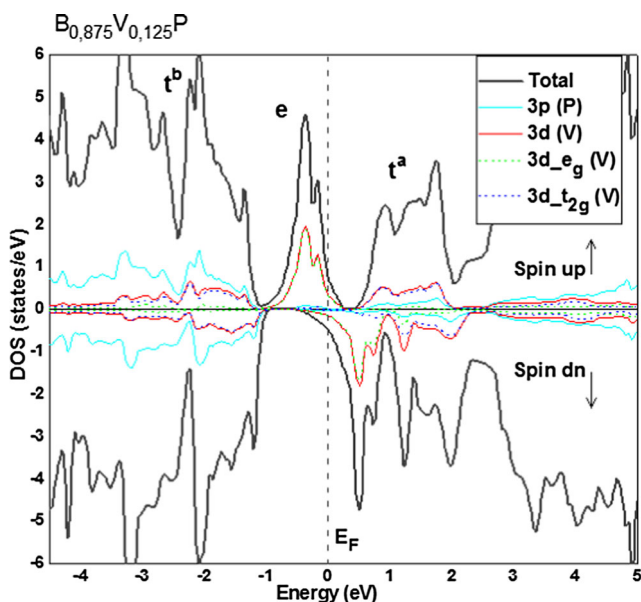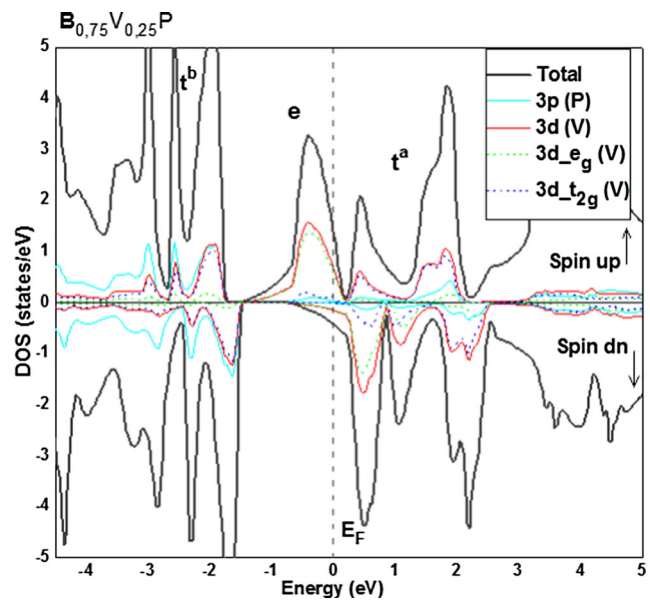
mechanism [58], that is well explained in the rule of Sato and Katayama-Yoshida. They have revealed that the stability of ferromagnetism in III-V DMSs have very similar chemical trends; they suggested that the ferromagnetic state is stable when delocalized t^a states are partially occupied [59]. However, in the case of $B_{1-x}V_xP$, when we examine their curves of TDOSs and PDOSs and the band structures (Figs. 5, 6, 7, 11, 12, 13), we note that the half-metallic behaviour is totally absent in all compounds. The substitution of the boron atom by vanadium cation in all $B_{1-x}V_xP$ DMSs at the tetrahedral environment is specific; this amounts to the chemical bonding system between the atoms. Bearing in mind the values of electro-negativities, that is about 2.04 and 2.19, respectively, for boron and phosphorus atoms on the scale of Pauling [60, 61] and on the Allred-Rochow scale of electro-negativities the boron marks the value of 2.01 that's closer in value of phosphorus which is 2.06 [62, 63]. These follow on a low hetero-polarity bond and, therefore automatically a low ionicity in the chemical bond B–P, that involves the sharing of electron pairs and done by the pooling between two electrons. The attractive potential of boron competes with that of the phosphorus atom to impose the valence charge. On the other hand, the chemical bond in the case of InP include a large ionic character than that of BP and formed by an ionic character bond system that is interpreted by electron transfer between the cationic and the anionic atoms. These two natures in formation of chemical bond between neighbouring atoms described with hybrid orbital have influence on the half-metallic behaviour of diluted magnetic semiconductors crystals.

Fig. 8 Spin-polarized band structures for majority spin (*up*) and minority spin (*dn*) for $In_{0.75}V_{0.25}P$. The Fermi level is set to zero (*dotted line*)
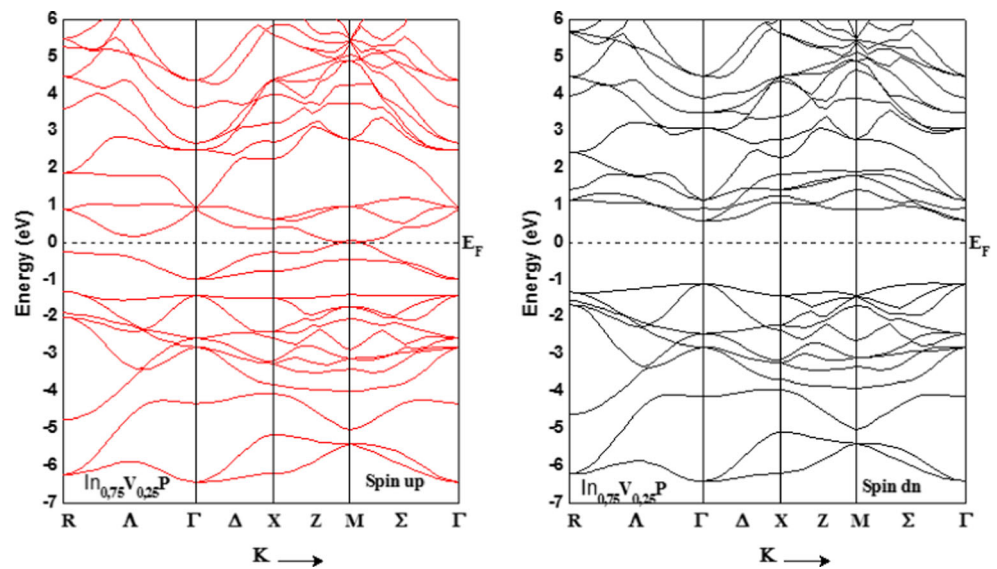
In these material class of DMSs, the electronic-state density 3d-eg and 3d-t2g of vanadium are not contributed similarly, it is clear that 3d-eg states are mainly participate in the non-bonding region (*e*) because it is fully occupied by two electrons and the completely empty of 3d-t2g level move the region of anti-bonding (t^a) beyond the Fermi level to create way for non-bonding state (*e*) near Fermi level. The 3d-eg states in the DMSs of indium phosphide $In_{1-x}V_xP$ at all concentrations have a powerful electronic density than that of boron phosphide $B_{1-x}V_xP$ DMSs. This can be interpreted by the little ionic character of the chemical bond B–P and the anionic potential that the boron atom can assume in the presence of vanadium. Therefore, the 3d-eg states of vanadium are coordinated both with the $3p$ state of phosphorus and the 2p states of boron in the case of $B_{1-x}V_xP$ that reduce its electronic density. Unlike the

DMSs of $In_{1-x}V_xP$, the 3d-eg of vanadium interact only with $3p$ state of phosphorus because it is the just atom that represent the anionic pole.

It is noted that the 3d-eg and 3d-t2g states contribute differently in the spin-up and the spin-down regions in the case of $In_{1-x}V_xP$, the majority spin states present a metallic effect because the minimum of the conduction band is situated at the Fermi level and the minority spin describe a clearly band gap at the Fermi level. The $In_{1-x}V_xP$ DMSs have the half-metallic ferromagnetic (HMF) behaviour that is a very important parameter in spintronic field; it is defined by the minima of the conduction band and maxima of the valence band and the absolute values of the highest energy of majority spin and (minority spin) valence bands. But in the case of $B_{1-x}V_xP$, the 3d-eg and 3d-t2g states have the same part in spin-up and spin-down. More than

Fig. 9 Spin-polarized band structures for majority spin (*up*) and minority spin (*dn*) for $In_{0.875}V_{0.125}P$. The Fermi level is set to zero (*dotted line*)

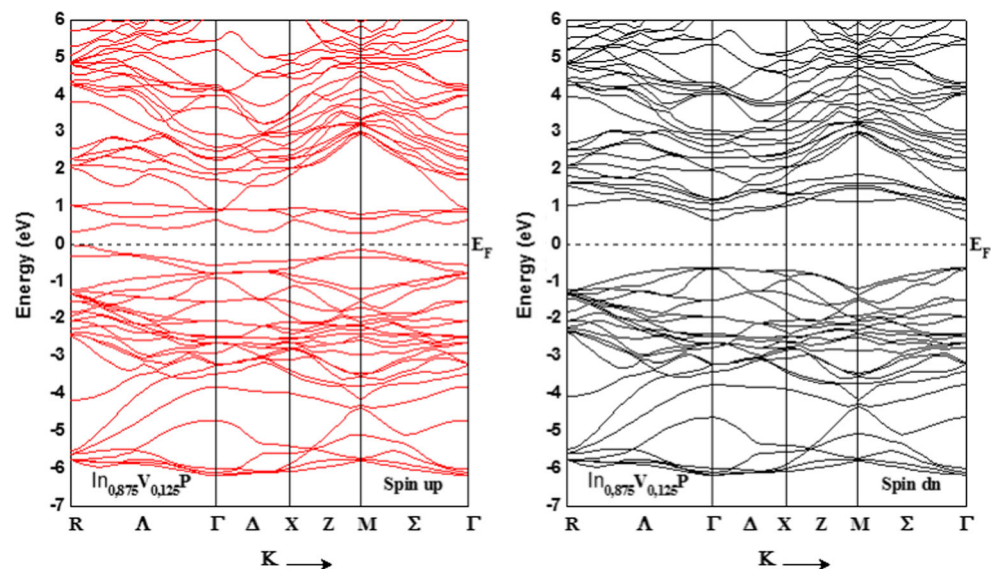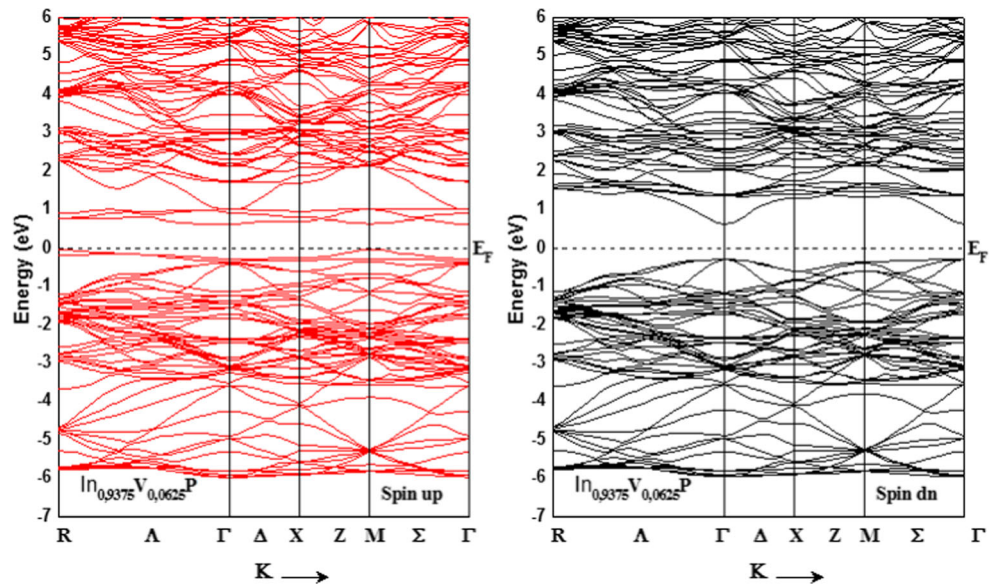**Fig. 10** Spin-polarized band structures for majority spin (*up*) and minority spin (*dn*) for $In_{0.9375}V_{0.0625}P$. The Fermi level is set to zero (*dotted line*)

the minimum of conduction band at all concentration of vanadium-doped boron phosphide DMSs located under the Fermi-level that gives a purely metallic ferromagnetic feature (FM) for all DMSs of $B_{1-x}V_xP$. We conclude that the insertion of vanadium in boron phosphide at all concentrations ignore the half-metallic ferromagnetic behaviour and limiting the using of $B_{1-x}V_xP$ DMSs in spintronic in contrast the DMSs of $In_{1-x}V_xP$ that is considered as a good candidates for spintronic applications.

According to Table 2, the $(B,In)_{1-x}V_xP$ have total magnetic moment of 2 μ_B (Bohr magneton), this magnetization is contributed differently between the interstitial site, phosphorus, vanadium, indium and boron atoms. The foremost proportion amounts to vanadium that contained two

unpaired electrons in the $3d$ state as cation V^{+3} with respect to the Hund's rule. We note that the magnetic moments of V, In and B atoms have the same sign whereas the smaller local magnetic moments from P atoms are negative in sign. It is explained by the fact that the valence band carriers in $3p$ states of phosphorus interact anti-ferromagnetically with vanadium spins. So, the origin of the magnetic moment in the case of $(B,In)_{1-x}V_xP$ is due essentially to vanadium.

In fact, from the band structures, we introduce two important parameters to describe the exchange splitting in DMSs alloys of $In_{1-x}V_xP$, the exchange constants $N_0\alpha$ (conduction band, CB) and the p–d exchange constant $N_0\beta$ (valence band, VB), these exchange constants can be determined by evaluating the spin-splitting of the conduction and the

Fig. 11 Spin-polarized band structures for majority spin (*up*) and minority spin (*dn*) for $B_{0.75}V_{0.25}P$. The Fermi level is set to zero (*dotted line*)

Fig. 12 Spin-polarized band structures for majority spin (*up*) and minority spin (*dn*) for $B_{0.875}V_{0.125}P$. The Fermi level is set to zero (*dotted line*)

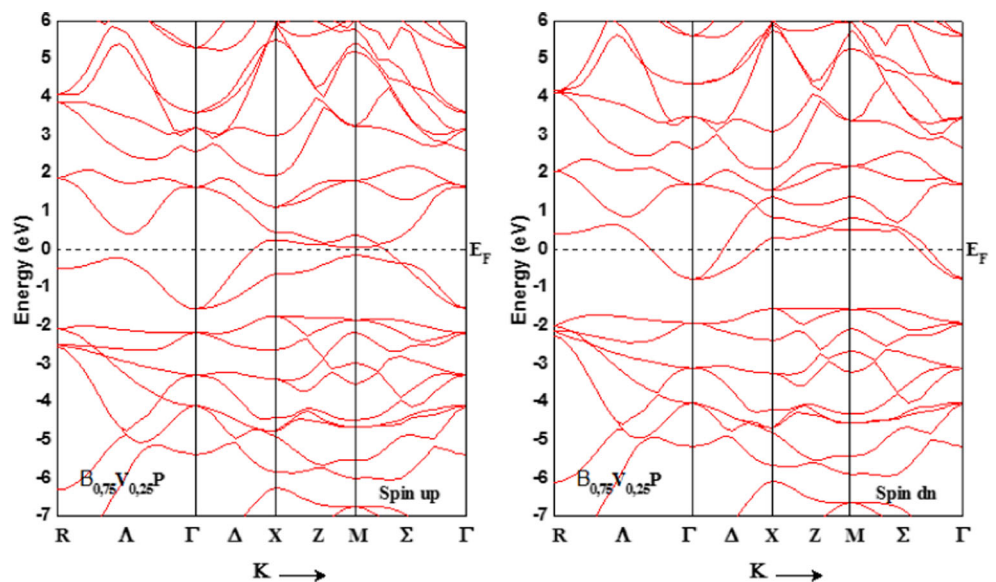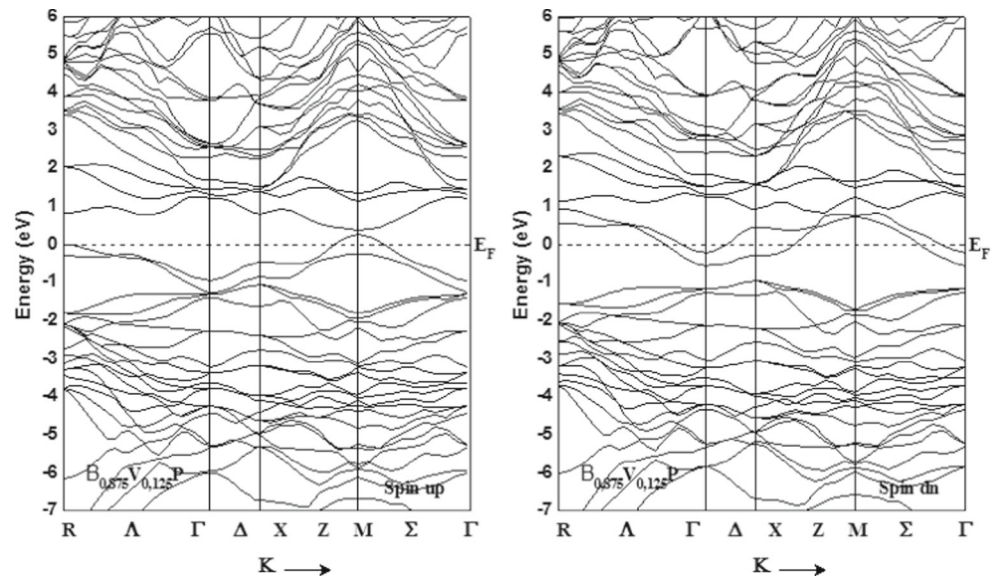**Fig. 13** Spin-polarized band structures for majority spin (*up*) and minority spin (*dn*) for $B_{0.9375}V_{0.0625}P$. The Fermi level is set to zero (*dotted line*)
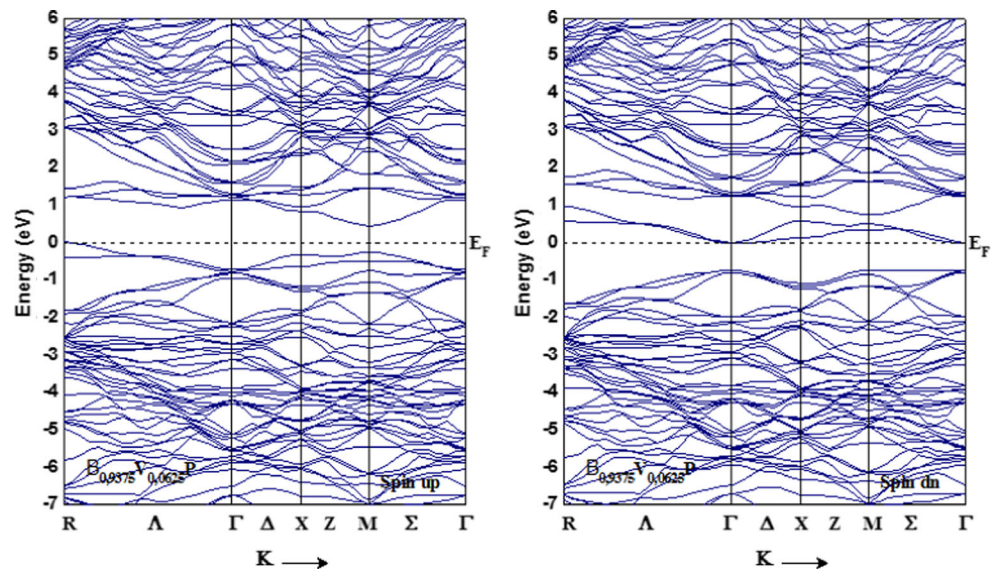

Table 2 Calculated half-metallic ferromagnetic band gap E_g and half-metallic gap G_h of minority spin, total and local magnetic moment (in Bohr magneton μ_B) within the muffin-tin spheres and in the interstitial sites and exchange constants $N_0\alpha$ and $N_0\beta$ for $(B,In)_{1-x}V_xP$ at concentrations ($x = 0.0625, 0.125, 0.25$)

| Compound | Concen. (x) | Energy gap (eV) | | | Moment magnetic (μB) | | | | Exchange constant | |
		E_g	G_h	Character	Interstitial	V	P	Total	$N_0\alpha$	$N_0\beta$
$In_{1-x}V_xP$	0.0625	0.913	0.321	HMF	0.338	1.886	−0.225	2	1.184	−1.525
	0.125	1.829	0.614	HMF	0.256	1.914	−0.173	2	3.111	−2.828
	0.25	1.517	0.725	HMF	0.268	1.855	−0.121	2	2.259	−5.108
$B_{1-x}V_xP$	0.0625			MF	0.734	0.957	−0.015	1.99		
	0.125			MF	0546	0.967	−0.012	1.78		
	0.25			MF	0.503	1.056	−0.002	1.77		

valence bands directly from the following mean-field theory expressions [57, 64]:

$$N_0\alpha = \frac{\Delta E_c}{x\langle s \rangle}$$

$$N_0\beta = \frac{\Delta E_v}{x\langle s \rangle}$$

where $\Delta E_c = E_c^{\downarrow} - E_c^{\uparrow}$ is the conduction band-edge spin-splitting and $\Delta E_v = E_v^{\downarrow} - E_v^{\uparrow}$ is the valence band-edge spin-splitting at the Γ symmetry point, (x) is the where (x) is the concentration of vanadium and $\langle s \rangle$ is half of the computed magnetization per V ion [65]. It is noticed that the values of p–d exchange splitting $N_0\beta$ and s–p exchange constants $N_0\alpha$ have opposite sign and the magnetic contribution from p–d interaction is slightly stronger than the s–d interaction. This is attributed to the fact that the exchange coupling between VB and $3d$-V is anti-ferromagnetic but it is ferromagnetic between CB and $3d$-V and means that the $In_{1-x}V_xP$ DMSs at various concentrations exhibit really a ferromagnetic feature.

4 Conclusion

The $(B,In)_{1-x}V_xP$ compounds at concentration $x = 0.0625$, 0.125 and 0.25 in zinc-blend phase have been studied by the FP-LAPW method to investigate their structural, electronic and magnetic properties. The results of PDOSs and TDOSs and the band structures confirm that the $In_{1-x}V_xP$ are half-metallic ferromagnetic with 100% spin polarization. Both Zener's double-exchange and p–d hybridization mechanism are responsible for ferromagnetic stabilization. Therefore, the $In_{1-x}V_xP$ alloys appear to be good candidates for spintronic applications. In the case of $B_{1-x}V_xP$, the half-metallic ferromagnetic character is totally absent because the smaller ionic character of the chemical bond in BP semiconductors that give week hybridization between $3d$ (V) and $3p$ (B).

References

1. Sze, S.M., Kwok, K.Ng.: Physics of semiconductor devices, 3rd Edition. Wiley (2007)
2. Oktyabrsky, S., Peide, D.Ye.: Fundamentals of III-V semiconductor MOSFETs. Springer (2010)
3. Furdyna, J.K.: J. Appl. Phys. **64**, R29 (1988)
4. Wolf, S.A., Awschalom, D.D., Buhrman, R.A., Daughton, J.M., Von Molnar, S., Roukes, M.L., Chtchelk-anova, A.Y., Treger, D.M.: Science **294**, 1488 (2001)
5. Kittel, C.: Introduction to solid state physics, 8th edition, Wiley (2005)
6. Cohen, M.L., Chelikowsky, J.R.: Electronic structure and optical properties of semiconductors. Springer (1988)
7. Becquerel, E.: Compt. Rendus **9**, 561 (1839)
8. Hertz, H.: Ann. Phys. **267**, 983 (1887)
9. Hayashi, T., Tanaka, M., Seto, K., Nishinaga, T., Ando, K.: Appl. Phys. Lett. **71**, 1825 (1997)
10. Ohno, H.: Science **281**, 951 (1998)
11. Dietl, T., Ohno, H., Matsukura, F., Cibert, J., Ferrand, D.: Science **287**, 1019–22 (2000)
12. Matsuda, A., Akiba, S.: Thin Solid Films **516**, 3873.3705–4366 (2008)
13. Miah, M.I., Gray, E.M.: Solid. State. Sci. **10**, 205 (2008)
14. Pei, G.Q., Xia, C.T., Dong, Y.J., Wu, B., Wang, T., Xu, J.: Scr. Mater. **58**, 943 (2008)
15. Munekata, H., Ohno, H., von Molnar, S., Segmiiller, A., Chang, L.L., Esaki, L.: Phys. Rev. Lett. **63**, 1849 (1989)
16. Munekata, H., Ohno, H., von Molnar, S., Harwit, A., Segmtiller, A., Chang, L.L.: J. Vat. Sci. Tech. B **8**, 176 (1990)
17. Von Molnar, S., Munekata, H., Ohno, H., Chang, L.L.: European MRS Meeting, Strasbourg (1990)
18. Ohno, H., Munekata, H., Penney, T., Von Molnar, S., Chang, L.L.: Phys. Rev. Lett. **68**, 2664 (1992)
19. Ohno, H., Shen, A., Matsukura, F., Oiwa, A., Endo, A., Katsumoto, S., Iye, Y.: Appl. Phys. Lett. **69**, 363 (1996)
20. Koshihara, S., Oiwa, A., Hirasawa, M., Katsumoto, S., Iye, Y., Urano, C., Takagi, H., Munekata, H.: Phys. Rev. Lett. **78**, 4617 (1997)
21. Dietl, T., Ohno, H., Matsukura, F., Cibert, J., Ferrand, D.: Science **287**, 1019 (2000)
22. Sajjad, M., Alay-e-Abbas, S.M., Zhang, H.X., Noor, N.A., Saeed, Y., Shakir, I., Shaukatet, A.: J. Magn. Magn. Mater. **390**, 78–86 (2015)
23. Kervan, S., Kervan, N.: J. Magn. Magn. Mater **382**, 63–70 (2015)
24. Boutaleb, M., Doumi, B., Tadjer, A., Sayede, A.: J. Magn. Magn. Mater **397**, 132–138 (2016)
25. Boutaleb, M., Doumi, B., Sayede, A., Tadjer, A., Mokaddem, A.: J. Supercond. Nov. Magn. **28**, 143–150 (2015)
26. Liang, P., Yang, L., Hu, X., Wang, L., Dong, Q., Jing, X.: J. Magn. Magn. Mater. **355**, 295–299 (2014)
27. Merabet, M., Rached, D., Benalia, S., Reshak, A.H., Bettahar, N., Righi, H., Baltache, H., Soyalp, F., Labair, M.: Superlattice. Microst. **65**, 195–205 (2014)
28. Boutaleb, M., Tadjer, A., Doumi, B., Djedid, A., Yakoubi, A., Dahmane, F., Abbar, B.: J. Supercond. Nov. Magn. **27**, 1603 (2014)
29. Dahmane, F., Tadjer, A., Doumi, B., Mesri, D., Aourag, H., Sayede, A.: Mater. Sci. Semicond. Proc. **21**, 66–73 (2014)
30. Doumi, B., Mokaddem, A., Sayede, A., Boutaleb, M., Tadjer, A., Dahmane, F.: J. Supercond. Nov. Magn. **28**(10), 3163–3172 (2015)
31. Cherfi, Y., Mokaddem, A., Bensaid, D., Doumi, B., Sayede, A., Dahmane, F.: J. Supercond. Nov. Magn. **29**, 1813–1817 (2016)
32. Zhang, Y.: J. Magn. Magn. Mater. **342**, 35–37 (2013)
33. Yao, G., Fan, G., Xing, H., Zheng, S., Ma, J., Zhang, Y., He, L.: J. Magn. Magn. Mater. **331**, 117–121 (2013)
34. Sharma, V., Manchanda, P., Sahota, P.K., Skomski, R., Kashyap, A.: J. Magn. Magn. Mater. **324**, 786–791 (2012)
35. Souissi, M., Schmerber, G., Derory, A., El Jani, B.: J. Magn. Magn. Mater. **324**, 2539–2542 (2012)
36. Wang, S.Q., Ye, H.Q.: Phys. Rev. B **66**, 235111 (2002)
37. Gorodynskyy, V., Zdansky, K., Pekarek, L., Malina, V., Vackova, S.: Nucl. Instr. Meth. A **555**, 288 (2005)
38. Bouarissa, N.: Phys. B: Condens. Matter **406**, 13.2583–2587 (2013)
39. Dietl, T., Ohno, H., Matsukura, F., Cibert, J., Ferrand, D.: Science **287**, 1019 (2000)
40. Schmidt, T.M., Venezuela, P., Arantes, J.T., Fazzio, A.: Phys. Rev. B **73**, 235330 (2006)

41. Hollingsworth, J., Bandaru, P.R.: Mater. Sci. Eng. B **151**, 152 (2008)
42. Udagawa, T.: Brevet US6809346, Boron phosphide-based semiconductor light-emitting device (2004)
43. Kumashiro, Y., Mitsuhashi, T., Okaya, S., Muta, F., Koshiro, T., Takahashi, Y., Mirabayashi, M.: Thermal conductivity of a boron phosphide single-crystal wafer up to high temperature. J. Appl. Phys. **65**, 2147 (1989)
44. Hohenberg, P., Kohn, W.: Phys. Rev. B **136**, 864 (1964)
45. Kohn, W., Sham, L.J.: Phys. Rev. A **140**, 1133 (1965)
46. Blaha, P., Schwarz, K., Madsen, G.K.H., Kvasnicka, D., Luitz, J.: WIEN2k, An augmented plane wave plus local orbitals program for calculating crystal properties. Vienna University of Technology, Vienna (2001)
47. Wu, Z., Cohen, R.E.: Phys. Rev. B **73**, 235116 (2006)
48. Monkhorst, H.J., Pack, J.D.: Phys. Rev. B **13**, 5188 (1976)
49. Pack, J.D., Monkhorst, H.J.: Phys. Rev. B **16**, 1748 (1977)
50. Muranghan, F.D.: Proc. Natl. Acad. Sci. USA **30**, 244 (1944)
51. Tran, F., Laskowski, R., Blaha, P., Schwarz, K.: Phys. Rev. B **75**, 115131 (2007)
52. Heyd, J., Peralta, J.E., Scuseria, G.E., Martin, R.L.: J. Chem. Phys. **123**, 174101 (2005)
53. Wyckoff, R.W.G. Crystal structures, 2nd edn. Krieger, Malabar (1986)
54. Liu, B.G.: Phys. Rev. B **67**, 172411 (2000)
55. Xu, Y.Q., Liu, B.G., Pettifor, D.G.: Phys. Rev. B **66**, 184435 (2002)
56. Yao, K.L., Gao, G.Y., Liu, Z.L., Zhu, L.: Solid State Commun. **133**, 301 (2005)
57. Gao, G.Y., Yao, K.L., Sasioglu, E., Sandratskii, L.M., Liu, Z.L., Jiang, J.L.: Phys. Rev. B **75**, 174442 (2007)
58. Akai, H.: Phys. Rev. Lett. **81**, 3002 (1998)
59. Sato, K., Katayama-Yoshida, H.: Semicond. Sci. Technol. **17**, 367–376 (2002)
60. Zumdahl Steven, S.: Chemical principles. 5th Edition. Chapter 13.2, Electronegativity pp. 587–590. Houghton Mifflin Company (2005)
61. Housecroft Catherine, E.: Inorganic Chemistry. 3rd Edition. Chapter 2.5, Electronegativity Values. pp. 42–44 Pearson Education Limited (2008)
62. Allred, A.L., Rochow, E.G.: J. Inorg. Nucl. Chem. **5**, 264 (1958)
63. Leroy, G.W. Organic chemistry, 7th edn. Pearson Education, Harlow (2006)
64. Raebiger, H., Ayuela, A., Nieminen, R.M.: J. Phys. Condens. Matter **16**, L457 (2004)
65. Sanvito, S., Ordejon, P., Hill, N.A.: Phys. Rev. B **63**, 165206 (2001)